

## Determination of $^{77}\text{Se}$ – $^{77}\text{Se}$ and $^{77}\text{Se}$ – $^{13}\text{C}$ $J$ -Coupling Parameters for the Clusters $[\text{Re}_5\text{OsSe}_8(\text{CN})_6]^{3-}$ and $[\text{Re}_4\text{Os}_2\text{Se}_8(\text{CN})_6]^{2-}$

Kannan Ramaswamy, Eric G. Tulsky,<sup>†</sup> Jeffrey R. Long,<sup>†</sup> Jeff L.-F. Kao, and Sophia E. Hayes\*

Department of Chemistry and Center for Materials Innovation, Washington University, St. Louis, Missouri 63130

Received August 18, 2006

We have investigated rarely observed  $^{77}\text{Se}$   $J$ -couplings (spin–spin couplings) in the mixed-metal face-capped octahedral clusters  $[\text{Re}_5\text{OsSe}_8(\text{CN})_6]^{3-}$  and  $[\text{Re}_4\text{Os}_2\text{Se}_8(\text{CN})_6]^{2-}$  at natural abundance. To the best of our knowledge, these are the first observations of Se–Se spin–spin interactions between  $\mu_3$ -Se sites, important for stereochemical assignments in hexarhenium analogues, Chevrel phase materials, and similar cluster materials. NMR techniques such as COSY, INADEQUATE, and 2D  $J$ -resolved spectroscopy have been used in conjunction to study these interactions. The two isomers (cis and trans) of  $[\text{Re}_4\text{Os}_2\text{Se}_8(\text{CN})_6]^{2-}$  were distinguishable, and selective isotopic labeling of  $[\text{Re}_5\text{OsSe}_8(\text{CN})_6]^{3-}$  with  $^{13}\text{C}$  ligands enabled resonances to be assigned by observing the  $^2J$  (Se–M–C) couplings. For  $[\text{Re}_5\text{OsSe}_8(\text{CN})_6]^{3-}$ , two different  $^2J$  (Se–M–Se) couplings were measurable on a single cluster, and these are related to one another through spin–spin interactions across a face diagonal or along an edge of the cube of inner selenium ligands. A rigorous analysis based on combinatorial math has been invoked to assign the couplings on the basis of the probability of multiple-spin interactions. The face diagonal association is found to result in a  $J$ -coupling interaction larger in magnitude than that from coupling along an edge of the cube—information critical for making stereochemical assignments of selenium sites.

### Introduction

$^{77}\text{Se}$  NMR spectroscopy is rapidly becoming an important analytical technique for the study of selenium in both inorganic and organic chemical structures.<sup>1</sup> While Se–Se  $J$ -couplings have been measured for organic<sup>2</sup> and inorganic polychalcogenides,<sup>3</sup> these are nonetheless very rare examples in the literature, despite the fact that  $^{77}\text{Se}$  NMR has been

reported in over 1100 publications.<sup>4</sup> To our knowledge, there have been only two previous reports of  $^{77}\text{Se}$ – $^{77}\text{Se}$   $J$ -coupling through a transition metal, M.<sup>5</sup> Such couplings are a key component for assignment of species in complex mixtures and would aid significantly in characterization. For example, a recent paper could not discriminate between different  $\text{Mo}_6$  chalcobromide isomers, illustrating the utility for such  $^{77}\text{Se}$   $J$ -couplings in making definitive assignments of resonances.<sup>6</sup> Studies of  $^{77}\text{Se}$ – $^{77}\text{Se}$   $J$ -couplings are therefore a useful and necessary component to complement other NMR analyses.

Our interest in  $^{77}\text{Se}$  NMR spectroscopy has been prompted by its potential for its use as a structural characterization tool. Selenium-77 is a spin-1/2 nucleus with a natural abundance of 7.58% and a very broad chemical shift range, making it an ideal probe of local chemical environments. We report here  $^{77}\text{Se}$  NMR studies on octahedral clusters of

\* To whom correspondence should be addressed. Tel: +1 (314) 935-4624. Fax: +1 (314) 935-4481. E-mail: hayes@wustl.edu.

<sup>†</sup> Department of Chemistry, University of California, Berkeley, CA 94720-1460.

- (1) (a) Duddeck, H. *Prog. Nucl. Magn. Reson. Spectrosc.* **1995**, *27*, 1–363. (b) Duddeck, H. *Ann. Rep. Nucl. Magn. Reson.* **2004**, *52*, 115–166.
- (2) See for example, Bhattacharyya, P.; Slawin, A. M. Z.; Woollins, J. D. *J. Chem. Eur.* **2002**, *8*, 2705–2711. Tonkikh, N.; Duddeck, H.; Petrova, M.; Neilands, O.; Strakovs, A. *Eur. J. Org. Chem.* **1999**, 1585–1588. Bates, M. C.; Morley, C. P. *J. Organomet. Chem.* **1997**, *533*, 193–196.
- (3) See for example, (a) Bergholdt, A. B.; Horn, E.; Takahashi, O.; Sato, S.; Kobayashi, K.; Furukawa, N.; Yokoyama, M.; Yamaguchi, K. *J. Am. Chem. Soc.* **1998**, *120*, 1230–1236. (b) Matsubayashi, G.; Yokozawa, A. *Inorg. Chim. Acta* **1993**, *208*, 95–97. (c) Björqvinnson, M.; Schrobilgen, G. *J. Inorg. Chem.* **1991**, *30*, 2540–2547. (d) Pekonen, P.; Hiltunen, Y.; Laitinen, R. S.; Pakkanen, T. A. *Inorg. Chem.* **1991**, *30*, 3679–3682. (e) Eggert, H.; Nielsen, O.; Henriksen, L. *J. Am. Chem. Soc.* **1986**, *108*, 1725–1730.

(4) Citations listed in SciFinder Scholar database, version 2006, American Chemical Society.

- (5) (a) Batchelor, R. J.; Einstein, F. W. B.; Gay, I. D.; Gu, J.-H.; Pinto, B. M. *J. Organomet. Chem.* **1991**, *411*, 147–157. (b) Ansari, M. A.; Chau, C.-N.; Mahler, C. H.; Ibers, J. A. *Inorg. Chem.* **1989**, *28*, 650–654.
- (6) Cordier, S.; Naumov, N. G.; Salloum, D.; Paul, F.; Perrin, C. *Inorg. Chem.* **2004**, *43*, 219–226.

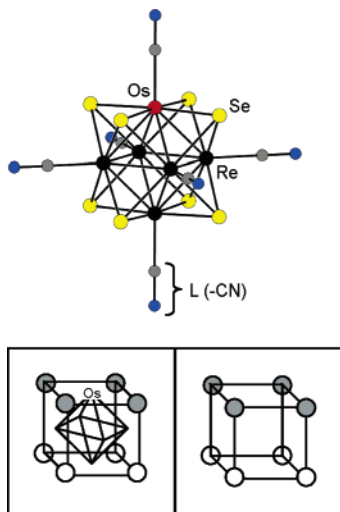


**Figure 1.** Structure and schematic representations of the face-capped octahedral cluster  $[\text{Re}_5\text{OsSe}_8(\text{CN})_6]^{3-}$ , which has  $C_{4v}$  symmetry. Note in the bottom schematic drawings that the eight inner selenium ligands form a cube with two types of sites: those associated with the osmium atom (gray spheres) and those that are not (white spheres). The outer ligands, L, are not shown.

the type  $\text{M}_6\text{Se}_8\text{L}_6$ , where M is a transition metal such as Mo or Re and L can be a variety of terminal ligands.<sup>7</sup> The basic structure type for these clusters consists of a central  $\text{M}_6$  octahedron, with eight surrounding selenium atoms, one capping each triangular face in a symmetric  $\mu_3$ -bonding arrangement. In addition to the selenium “inner ligands,” each metal site is capped by a radially extending “outer ligand,” L. Thus, the cluster exhibits the full symmetry of an octahedron, with all eight inner ligands (Se) and all six outer ligands (L) equivalent, and the  $^{77}\text{Se}$  NMR spectrum would be expected to contain one singlet.

The clusters under investigation here,  $[\text{Re}_5\text{OsSe}_8(\text{CN})_6]^{3-}$  and  $[\text{Re}_4\text{Os}_2\text{Se}_8(\text{CN})_6]^{2-}$ , differ from this basic structure in that the octahedral symmetry of the cluster has been lowered, presenting an opportunity for more detailed NMR investigations. For  $[\text{Re}_5\text{OsSe}_8(\text{CN})_6]^{3-}$  (hereafter termed “ $\text{Re}_5\text{Os}$ ”), one rhenium atom in the central octahedron has been replaced by an osmium atom, lowering the symmetry to  $C_{4v}$ , as shown in Figure 1. The eight selenium atoms are then separated into two chemically inequivalent sites: four equivalent atoms cap triangular faces of  $\text{Re}_3$ , while the other four cap  $\text{Re}_2\text{Os}$  faces. In addition, the outer cyanide ligands are no longer equivalent: one cyanide caps an osmium center, four cap the equatorial rhenium sites, and one caps the rhenium positioned trans to the osmium atom.

For  $[\text{Re}_4\text{Os}_2\text{Se}_8(\text{CN})_6]^{2-}$ , hereafter termed “ $\text{Re}_4\text{Os}_2$ ”, two rhenium sites in the central octahedron have been replaced

with osmium.<sup>8</sup> This further complicates the situation because now two isomers form, one where osmium atoms occupy trans vertices of the octahedron, resulting in  $D_{4h}$  symmetry, and one with osmium at cis vertices, producing  $C_{2v}$  symmetry (see Figure 2). In the trans isomer (Figure 2a), all eight selenium atoms are equivalent, while two types of cyanide ligand are present—the four bound to rhenium and the two bound to osmium. The lower symmetry of the cis isomer (Figure 2b) means there are three chemically inequivalent selenium sites (two atoms capping  $\text{ReOs}_2$  faces, four capping  $\text{Re}_2\text{Os}$  faces, and two capping  $\text{Re}_3$  faces) and three chemically inequivalent cyanide ligands (two bound to osmium, two bound to rhenium atoms cis to the osmium, and two bound to rhenium atoms trans to the osmium).

Given the 7.58% natural abundance of  $^{77}\text{Se}$ , a simple metal complex with only two selenium atoms would scarcely exhibit  $J$ -coupling, as only  $0.0758 \times 0.0758 = 0.575\%$  of the complexes would have the two NMR-active  $^{77}\text{Se}$  isotopes at both selenium sites. However, the eight selenium sites present in the  $\text{M}_6\text{Se}_8$  clusters considered here make measuring such coupling much easier, as finding two  $^{77}\text{Se}$  nuclei out of eight sites is much more probable than when we had only two sites to choose from.<sup>9</sup> Indeed, 10.0% of the clusters will have two  $^{77}\text{Se}$  atoms, 1.64% of the clusters will have three, and just 0.167% will have four or more, while 34.9% will have only one  $^{77}\text{Se}$  NMR-active spin. The balance of the clusters ( $\sim 53\%$ ) has no NMR-active selenium and will therefore not be observed in our experiments. As a result, fully 11.8% of the clusters will produce  $^{77}\text{Se}$  NMR spectra with multiple NMR-active nuclei, making this an ideal system for the measurement of  $^{77}\text{Se}-\text{M}-^{77}\text{Se}$   $J$ -coupling.

Herein, we demonstrate an experimental methodology for probing these  $J$ -coupling interactions and observing them in one- and two-dimensional NMR experiments. Specifically, we utilize these chalcocyanide clusters as a prototype in establishing experiments for resolving such interactions, thereby laying a foundation for future studies of other systems with multiple types of selenium sites.

## Experimental Section

Solid samples of  $(\text{Bu}_4\text{N})_3[\text{Re}_5\text{OsSe}_8(\text{CN})_6]$  and  $(\text{Bu}_4\text{N})_2[\text{Re}_4\text{Os}_2\text{Se}_8(\text{CN})_6]$  were synthesized by previously reported procedures.<sup>8</sup> The former was recrystallized at least three times by diffusion of ether vapor into a concentrated acetonitrile solution, while the latter was recrystallized by diffusion of ether vapor into a concentrated dichloromethane solution. The recrystallized solids were dissolved in a 3:1 mixture of dimethylformamide (DMF) and  $d$ -DMF for NMR analyses; all samples were degassed to remove oxygen prior to measurement.  $^{77}\text{Se}$  NMR experiments were recorded using a Varian Inova-500 spectrometer equipped with a Nalorac broadband 10 mm probe at 95.3 MHz. All  $^{77}\text{Se}$  experiments were referenced

(7) (a) Saito, T.; Yamamoto, N.; Nagase, T.; Tsuboi, T.; Kobayashi, K.; Yamagata, T.; Imoto, H.; Unoura, K. *Inorg. Chem.* **1990**, *29*, 764–770. (b) Long, J. R.; McCarty, L. S.; Holm, R. H. *J. Am. Chem. Soc.* **1996**, *118*, 4603–4616. (c) Mironov, Y. V.; Cody, J. A.; Albrecht-Schmitt, T. E.; Ibers, J. A. *J. Am. Chem. Soc.* **1997**, *119*, 493–498. (d) Hamard, C.; LeFloch, M.; Pena, O.; Wojakowski, A. *Physica B* **1999**, *259–261*, 701–702. (e) Mironov, Y. V.; Virovets, A. V.; Naumov, N. G.; Ikorskii, V. N.; Fedorov, V. E. *Chem. Eur. J.* **2000**, *6*, 1361–1365. (f) Roland, B. K.; Carter, C.; Zheng, Z. *J. Am. Chem. Soc.* **2002**, *124*, 6234–6235. (g) Gray, T. G.; Rudzinski, C. M.; Meyer, E. E.; Holm, R. H.; Nocera, D. G. *J. Am. Chem. Soc.* **2003**, *125*, 4755–4770.

(8) Tulskey, E. G.; Crawford, N. R. M.; Baudron, S. A.; Batail, P.; Long, J. R. *J. Am. Chem. Soc.* **2003**, *125*, 15543–15553.

(9) Eight possible Se sites are NMR-active. Let  $m = 8$  for the number of sites,  $n$  correspond to the number of NMR-active spins, and  $a$  is the isotopic abundance of the particular nucleus (in %). The probability of finding  $n$  NMR-active spins is  $P_n = (m!/(n!(m-n)!))(100\% - a)^{m-n}(a)^n$ . See, for example, Hoel, P. G.; Port, S. C.; Stone, C. J. *Introduction to Probability Theory*; Houghton Mifflin Company: Boston, 1971; p 21.

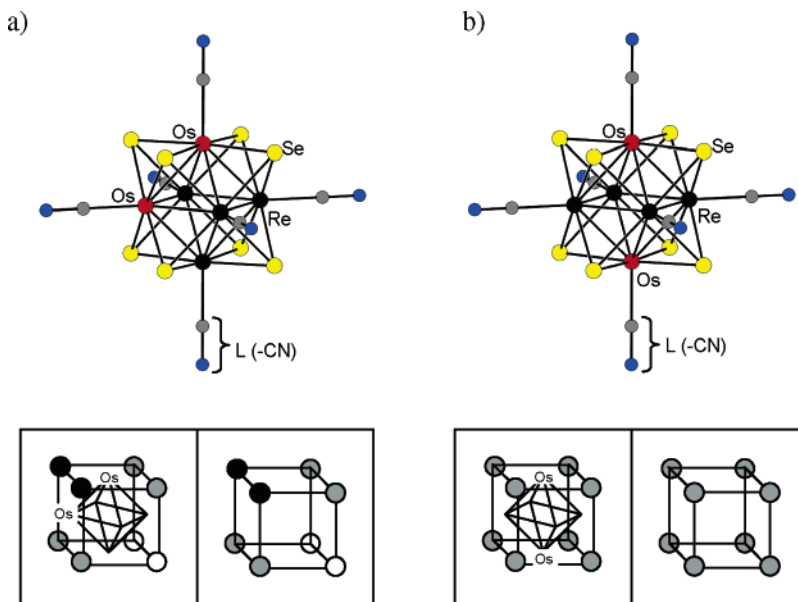


**Figure 2.** Structure and schematic representations of the face-capped octahedral clusters: (a) *trans*-[Re<sub>4</sub>Os<sub>2</sub>Se<sub>8</sub>(CN)<sub>6</sub>]<sup>2-</sup>, *D*<sub>4h</sub> symmetry, and (b) *cis*-[Re<sub>4</sub>Os<sub>2</sub>Se<sub>8</sub>(CN)<sub>6</sub>]<sup>2-</sup>, *C*<sub>2v</sub> symmetry. Note in the bottom schematic drawings that the eight inner selenium ligands are all equivalent for the *trans* isomer, whereas there are three chemically inequivalent Se sites on the *cis* cluster. The outer ligands, L, are not shown.

to a secondary reference standard, diphenyl selenide, with a resonance at 403 ppm relative to dimethyl selenide (the primary reference at 0 ppm) at 25 °C. The *T*<sub>1</sub> relaxation time at room temperature was 1.5 s.

A combination of <sup>77</sup>Se COSY, 2D *J*-resolved spectroscopy, and 1D double-quantum coherence (INADEQUATE) sequences were applied to fully reveal the details of the *J*-coupling interactions. The <sup>77</sup>Se COSY experiments were obtained with an 11.2 kHz spectral width and a 15.5 μs  $\pi/2$  pulse width. A data matrix with 4096 complex points in the F2 dimension and 256 real points in the F1 dimension was collected with 160 transients per *T*<sub>1</sub> increment. The <sup>77</sup>Se 2D *J*-resolved spectrum was recorded with 12.4 kHz in F2 and 200 Hz in the F1 dimension, respectively. The spectrum was collected in a data matrix of 4096 points in the F2 dimension and 128 points in the F1 dimension with 256 transients per each *T*<sub>1</sub> value. Finally, the one-dimensional double-quantum coherence experiment was recorded with an 18 μs  $\pi/2$  pulse and fixed evolution delays of 4.1 and 22.7 ms, equivalent to (4*J*<sub>SeSe</sub>)<sup>-1</sup> where *J*<sub>SeSe</sub> is approximately 60 and 11 Hz, respectively. These spectra were collected as 128k data points with ~50 000 transients.

Separate <sup>13</sup>C-labeled samples, (Bu<sub>4</sub>N)<sub>3</sub>[Re<sub>5</sub>OsSe<sub>8</sub>(<sup>13</sup>CN)<sub>6</sub>] and (Bu<sub>4</sub>N)<sub>2</sub>[Re<sub>4</sub>Os<sub>2</sub>Se<sub>8</sub>(<sup>13</sup>CN)<sub>6</sub>], were prepared with 98% <sup>13</sup>C-cyanide ligands. The <sup>13</sup>C spectra of these compounds were obtained with a 25 kHz spectral width collected as 64k data points. Approximately 7000 transients were recorded, with  $\pi/2$  pulses of 21 μs, at 125.89 MHz. The chemical shifts were measured in ppm downfield from tetramethylsilane (TMS). The spectra were recorded at 25 °C with a pre-acquisition delay of at least 5\**T*<sub>1</sub>.

Spectra were processed with a Bayesian fitting program<sup>10</sup> to deconvolute *J*-coupled features. Resonances were fit to extract chemical shifts, peak widths, and peak areas. When individual *J*-coupled satellites were not clearly resolved, a resolution enhancement window function was utilized. The free induction decay is multiplied by a weighting function:<sup>11</sup>  $f(t) = \exp[-(tl) - (t/g)^2]$  where *l* is the line broadening defined for the apodization function,

(10) Bretthorst, G. L. *J. Magn. Reson.* **1990**, *88*, 571–595.

(11) See, for example, Ernst, R. R.; Bodenhausen, G.; Wokaun A. *Principles of Nuclear Magnetic Resonance in One and Two Dimensions*; Clarendon Press: Oxford, 1994; p 108.

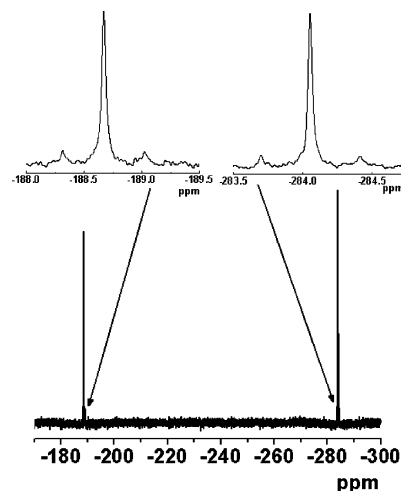


**Figure 3.** <sup>77</sup>Se spectrum of [Re<sub>5</sub>OsSe<sub>8</sub>(CN)<sub>6</sub>]<sup>3-</sup> in dimethylformamide. Insets are expanded views of the two features.

*g* is the Gaussian function time constant, and *t* is the acquisition time. Negative *l* values result in resolution enhancement to the spectrum; typical values used are indicated in the captions for each spectrum.

## Results

**Re<sub>5</sub>Os Cluster.** Two multiplets were observed in the Bloch decay (“1-pulse”) spectrum of [Re<sub>5</sub>OsSe<sub>8</sub>(CN)<sub>6</sub>]<sup>3-</sup> corresponding to the two chemically inequivalent types of selenium atoms. The <sup>77</sup>Se spectrum is shown in Figure 3. Integration indicates a ratio of peak areas of 1:1 (to within 3%), as expected for the two types of selenium sites present in each cluster (see Figure 1). At room temperature (21 °C), the chemical shifts of the two multiplets are centered at –188.6 and –284.0 ppm. The deshielded resonance at –188.6 ppm has been assigned to the  $\mu_3$ -Se species capping the Re<sub>2</sub>Os triangular faces, and the shielded resonance at –284.0 ppm to those  $\mu_3$ -Se species capping the Re<sub>3</sub> (see the

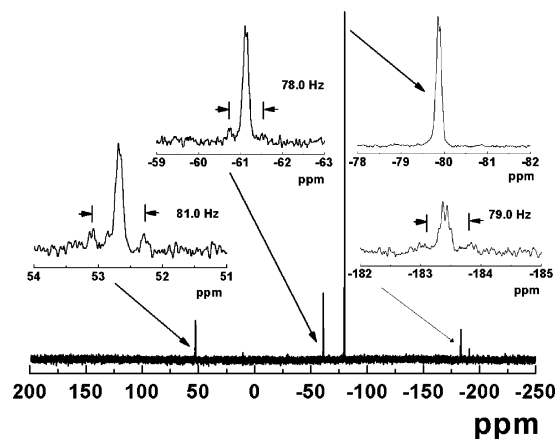


**Figure 4.**  $^{77}\text{Se}$  spectrum of  $[\text{Re}_4\text{Os}_2\text{Se}_8(^{13}\text{CN})_6]^{2-}$  in dimethylformamide. Insets are expanded views of the four features.

Discussion section for further details about the assignments). It is worthwhile to note that these chemical shifts are temperature dependent (changing  $\sim 0.06\text{--}0.08$  ppm/ $^\circ\text{C}$ ), so there is an uncertainty of  $\sim \pm 0.4$  ppm in the chemical shift depending on the precise sample temperature.

Each multiplet in the spectrum appears as a large resonance flanked by  $J$ -coupled satellites that are split by 67 Hz. The satellite intensities are relatively weak, and they are observed only after significant signal averaging (i.e., 3000 transients). Peak fitting of the two satellites yielded a relative area of  $\sim 11\text{--}12\%$  of the total peak area in the multiplet (see Discussion section below).

**$\text{Re}_4\text{Os}_2$  Cluster.** Two isomers of the  $[\text{Re}_4\text{Os}_2\text{Se}_8(\text{CN})_6]^{2-}$  cluster are present in solution, as evidenced by the  $^{77}\text{Se}$  Bloch decay spectrum shown in Figure 4. Four resonances are observed, and three of these exhibit  $J$ -coupled satellites, as apparent in the inset images. The samples employed were  $^{13}\text{C}$ -labeled species, and therefore, some fine structure due to  $^2J_{\text{Se-C}}$  couplings can also be seen in the insets. The one intense resonance at  $-79.9$  ppm is immediately assignable to the *trans*- $[\text{Re}_4\text{Os}_2\text{Se}_8(\text{CN})_6]^{2-}$  species, as it lacks  $J$ -coupled satellites. The other three resonances have intensities in a 1.1:2.7:1.0 ratio, in keeping with the expected 2:4:2 ratio shown in Figure 2b for the *cis*- $[\text{Re}_4\text{Os}_2\text{Se}_8(\text{CN})_6]^{2-}$  species. These peaks, occurring at 52.7,  $-60.9$ , and  $-182.5$  ppm, have been assigned to  $\mu_3$ -Se atoms capping the  $\text{ReOs}_2$ ,  $\text{Re}_2\text{Os}$ , and  $\text{Re}_3$  triangular faces, respectively. Integration of all resonances in the spectrum results in a ratio of total peak areas of 1.95:1.00 for the *trans* species to the *cis* species, consistent with the observation that the *trans* geometry is more stable under cluster formation conditions.<sup>12</sup> As in the  $\text{Re}_5\text{Os}$  cluster, these chemical shifts are temperature dependent, so there is an uncertainty of  $\sim \pm 0.4$  ppm in the chemical shift.

The small quantity of  $[\text{Re}_4\text{Os}_2\text{Se}_8(\text{CN})_6]^{2-}$  available prevented a more detailed analysis of the  $J$ -coupling in this species. Consequently, only the Bloch decay spectra ( $^{77}\text{Se}$  and  $^{13}\text{C}$ ) are presented herein.

**$J$ -Coupling.** Identification of the  $J$ -coupling interactions in  $[\text{Re}_5\text{OsSe}_8(\text{CN})_6]^{3-}$  was accomplished through a series of

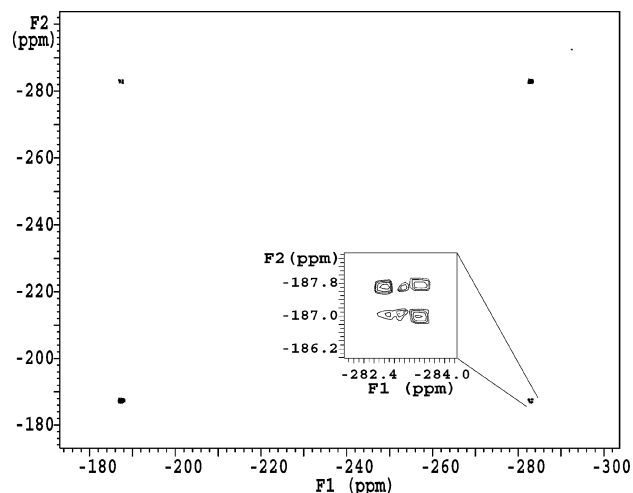


**Figure 5.**  $^{77}\text{Se}$  COSY spectrum of  $[\text{Re}_5\text{OsSe}_8(\text{CN})_6]^{3-}$  in dimethylformamide. Inset images are expansions of cross-peaks, as indicated.

experiments designed to selectively highlight these homonuclear spin–spin interactions, including COSY, 2D  $J$ -resolved spectroscopy, and 1D double-quantum coherence. COSY<sup>13</sup> is effective at analyzing homonuclear  $J$ -couplings because cross-peaks appear when spins are coupled to one another. Figure 5 shows the COSY spectrum recorded for the  $\text{Re}_5\text{Os}$  sample with the inset image showing an expanded cross-peak region. Here, couplings of 68 Hz are clearly resolved in the cross-peak multiplets. However, since this sample has the possibility for three distinct homonuclear Se–Se coupling interactions, there is some concern that overlapping multiplets might obscure important features. Two-dimensional  $J$ -resolved spectroscopy<sup>14</sup> is an experiment that addresses this concern; here, chemical shifts and  $J$ -couplings are separated and displayed on different axes.

Individual traces from the 2D  $J$ -resolved spectrum depicted in Figure 6 again show the  $J$ -coupled satellites split by 66–68 Hz. However, a second pair of satellites is now also visible, split by only 12–13 Hz. This weaker splitting is clearly visible but is not fully resolved from the strong central singlet arising from clusters containing only one  $^{77}\text{Se}$  nucleus.

The one-dimensional double-quantum coherence (INADEQUATE)<sup>15</sup> pulse sequence suppresses this central singlet to reveal occluded smaller features, with  $J$ -coupled resonances appearing as antiphase pairs. An INADEQUATE experiment with  $\sim 50\,000$  transients was collected and is shown in Figure 7; the large number of scans was necessary because of the lower sensitivity of this experiment compared to COSY or 2D  $J$ -resolved spectroscopy. The two pairs of coupled resonances appear as antiphase doublets, split by 67 Hz for the more intense outer pair and 10–11 Hz for the less intense inner pair. The spectrum shown is for a fixed evolution period, equivalent to  $(4J_{\text{SeSe}})^{-1}$ , of 4.1 ms; that for 22.7 ms is not shown. This spectrum provides an important complement to the features that were evident but not

(13) Aue, W. P.; Bartholdi, E.; Ernst, R. R. *J. Chem. Phys.* **1976**, *64*, 2229–2246.

(14) Aue, W. P.; Karhan, J.; Ernst, R. R. *J. Chem. Phys.* **1976**, *64*, 4226–4227.

(15) Bax, A.; Freeman, R.; Kempell, S. P. *J. Am. Chem. Soc.* **1980**, *102*, 4849–4851.

(12) Tulskey, E. G.; Long, J. R. *Inorg. Chem.* **2001**, *40*, 6990–7002.



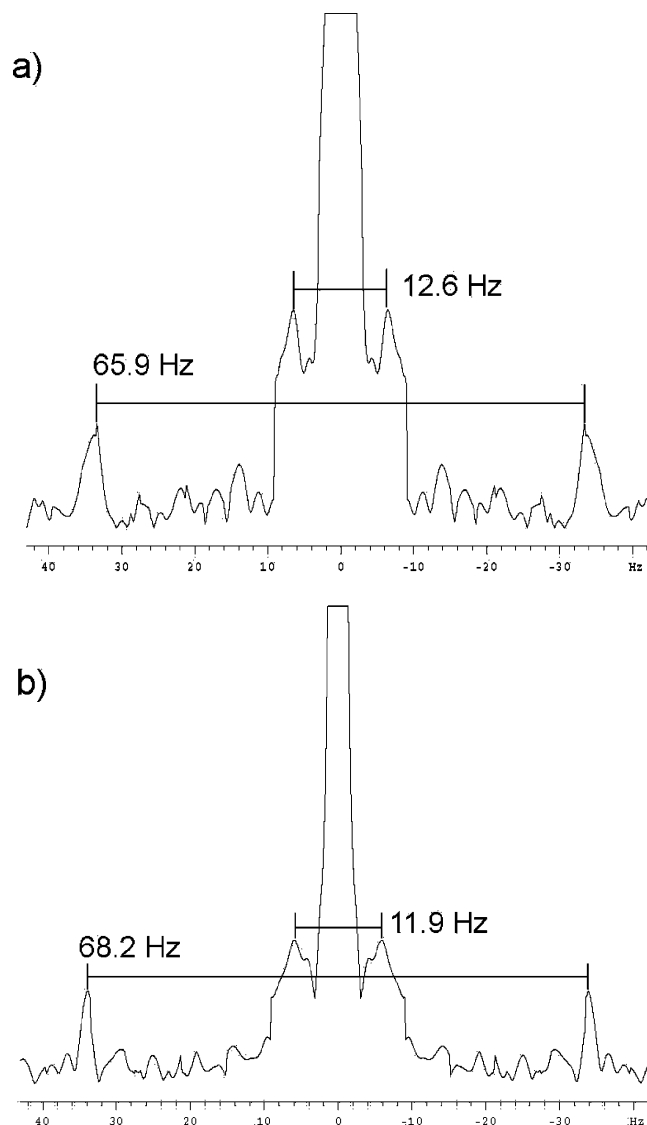


**Figure 6.** Traces from the 2D *J*-resolved  $^{77}\text{Se}$  spectrum of  $[\text{Re}_5\text{OsSe}_8(\text{CN})_6]^{3-}$ : (a) expanded trace of the multiplet at  $-188.6$  ppm and (b) expanded trace of the multiplet at  $-284.0$  ppm.

completely resolved in the 2D *J*-resolved spectra. The *J*-couplings resolved here are important features only visible in the INADEQUATE measurement that would not have been fully resolved otherwise.

A series of  $^{77}\text{Se}$  spectra were recorded on a  $^{13}\text{C}$ -labeled analogue to assist in assigning the  $\text{Re}_3$ -capped site and the  $\text{Re}_2\text{Os}$ -capped site while providing an opportunity for observing  $^{77}\text{Se}$ – $^{13}\text{C}$  *J*-couplings. The  $^{77}\text{Se}$  spectra for  $[\text{Re}_5\text{OsSe}_8(^{13}\text{CN})_6]^{3-}$  exhibit a fine-structured central resonance flanked by two satellites at 64 Hz, similar to those observed for the unlabeled cluster (see Figure 8a and b). The central multiplet for the more shielded resonance (at  $-281.8$  ppm in Figure 8b) appears as an approximate 1:3:3:1 quadruplet, confirmed by integration using the Varian VNMR program. The regularity of these features helped assign it to the  $\mu_3$ -Se species capping  $\text{Re}_3$  triangular faces. The quadruplet features are split by 6.0–6.7 Hz. These features are more easily observed in the spectrum to which negative line broadening has been applied (Figure 8d). The deshielded resonance (at  $-186.6$  ppm) has a less clear splitting pattern

(apparent as shoulders in Figure 8a but fully resolved in Figure 8c) with negative line broadening, as expected for the  $\mu_3$ -Se species capping  $\text{Re}_2\text{Os}$  triangular faces. The inner two resonances are split by 4.8 Hz, and the outer two satellites appear at separations of 5.4 and 5.6 Hz from the central pair.

A 2D *J*-resolved spectroscopy experiment was carried out on a solution containing  $[\text{Re}_6\text{Se}_8(\text{CN})_6]^{4-}$ ,<sup>16</sup> for which one would expect no *J*-coupling, since all eight selenium sites within the hexarhenium cluster are chemically equivalent. Indeed, no fine structure was observed for this sample (data not shown). Too little of the  $[\text{Re}_4\text{Os}_2\text{Se}_8(\text{CN})_6]^{2-}$  sample was available to observe Se–Se coupling features with accuracy. However, pairs of *J*-coupled satellites are evident for the three resonances attributable to *cis*- $[\text{Re}_4\text{Os}_2\text{Se}_8(\text{CN})_6]^{2-}$ . The relative magnitude of the couplings ranges from 78 to 81 Hz (see insets of Figure 4), which is slightly larger than similar satellites observed in the  $\text{Re}_5\text{Os}$  clusters.

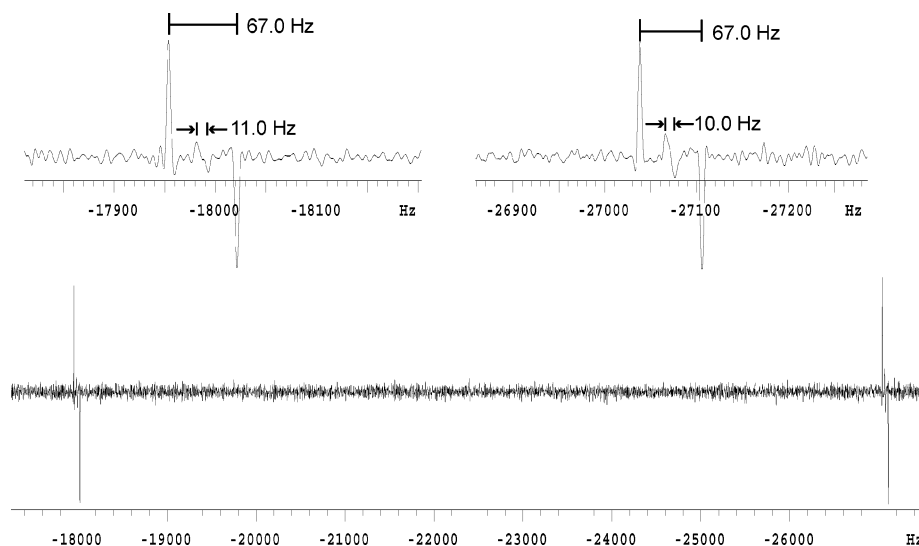
**$^{13}\text{C}$  NMR Spectra.** As expected, the  $^{13}\text{C}$  NMR spectrum of  $[\text{Re}_5\text{OsSe}_8(^{13}\text{CN})_6]^{3-}$  consists of three resonances with ratios of  $\sim 1:4:1$  (see Figure 9): at 113.5 ppm (resonance **x**) for carbon bound to the “axial” rhenium site trans to the osmium atom, at 112.2 ppm (resonance **y**) for carbon bound to the four equivalent “equatorial” rhenium sites, and at 97.7 ppm (resonance **z**) for carbon bound to osmium. Figure 10a displays an expansion of resonance **x**, which exhibits a conventional apodization line broadening (*l*) of 1 Hz; for comparison, Figure 10b shows the same region with negative line broadening. All three resonances were processed similarly, and satellites flanking each are now distinguishable. The magnitude of these splittings is indicated in the figure.

Figure 11 depicts the  $^{13}\text{C}$  spectrum of  $[\text{Re}_4\text{Os}_2\text{Se}_8(\text{CN})_6]^{2-}$  at natural abundance. Resonances from both *cis* and *trans* isomers of the cluster are evident. For the *trans* isomer, the two resonances have a ratio of 4:2, reflecting the cyanide species bound to four equivalent equatorial rhenium sites (106.7 ppm) versus two equivalent osmium sites trans to one another (92.3 ppm). The *cis* isomer has three resonances of nearly equal intensity, corresponding to the three pairs of chemically inequivalent cyanide ligands. Two cyanide ligands are bound to the two osmium atoms, giving rise to the resonance at 91.1 ppm. Out of the four remaining cyanides, two are bound to rhenium atoms that are *cis* to only one osmium atom (107.6 ppm), and two are bound to rhenium atoms that are *cis* to two osmium atoms (106.6 ppm). The chemical shift of the latter species is co-incident with that of the *trans* isomer, in which every rhenium atom is bound to two osmium atoms. As in the  $\text{Re}_5\text{Os}$  cluster, the most shielded cyanide resonances are those bound to osmium, as assigned by examining the relative ratios of the *trans* isomer.

## Discussion

**$^{77}\text{Se}$  NMR Spectrum of  $[\text{Re}_5\text{OsSe}_8(\text{CN})_6]^{3-}$  and  $J_{\text{SeSe}}$  Coupling.** From the Bloch decay spectrum, the deshielded multiplet centered at  $-188.6$  ppm is assigned to the  $\mu_3$ -Se

(16) Synthesis reported in Bennett, M. V.; Beauvais, L. G.; Shores, M. P.; Long, J. R. *J. Am. Chem. Soc.* **2001**, *123*, 8022–8023.



**Figure 7.** One-dimensional double-quantum coherence (INADEQUATE)  $^{77}\text{Se}$  spectrum of  $[\text{Re}_5\text{OsSe}_8(\text{CN})_6]^{3-}$  with a 4.1 ms fixed evolution period. (a) Expanded spectrum of the multiplet centered at  $-188.6$  ppm, (b) expanded spectrum of the multiplet centered at  $-284.0$  ppm, and (c) full spectrum showing both resonances.

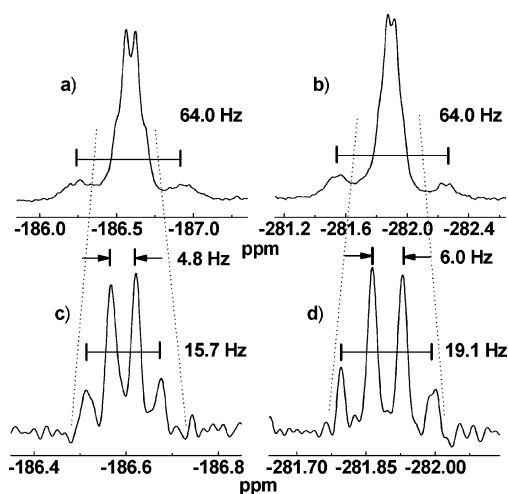


**Figure 8.**  $^{77}\text{Se}$  spectra of  $[\text{Re}_5\text{OsSe}_8(^{13}\text{CN})_6]^{3-}$  in dimethylformamide at  $37.5$  °C: (a) expanded spectrum of resonance centered at  $-186.6$  ppm, (b) expanded spectrum of resonance centered at  $-281.8$  ppm, (c) spectrum corresponding to (a) with negative line broadening, and (d) spectrum corresponding to (b) with negative line broadening ( $l = -5$ ,  $g = 0.2$ ).

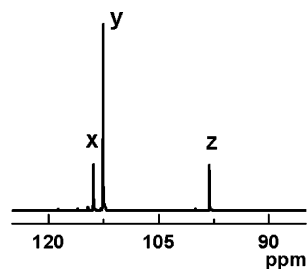


**Figure 9.**  $^{13}\text{C}$  spectrum of  $[\text{Re}_5\text{OsSe}_8(^{13}\text{CN})_6]^{3-}$  in DMF (without  $^1\text{H}$  decoupling). Resonance **x** is assigned to  $-\text{CN}$  bound to rhenium in the “axial” position located trans to osmium. Resonance **z** is assigned to  $-\text{CN}$  bound to the osmium, and resonance **y** to the four  $-\text{CN}$  species bound to the four equivalent “equatorial” rhenium positions.

species capping the  $\text{Re}_2\text{Os}$  triangular faces, while the shielded multiplet at  $-284.0$  ppm is assigned to those capping the  $\text{Re}_3$  faces. The assignments were made by observing the  $J_{\text{SeC}}$  couplings in the  $^{13}\text{C}$  spectra, as described below.

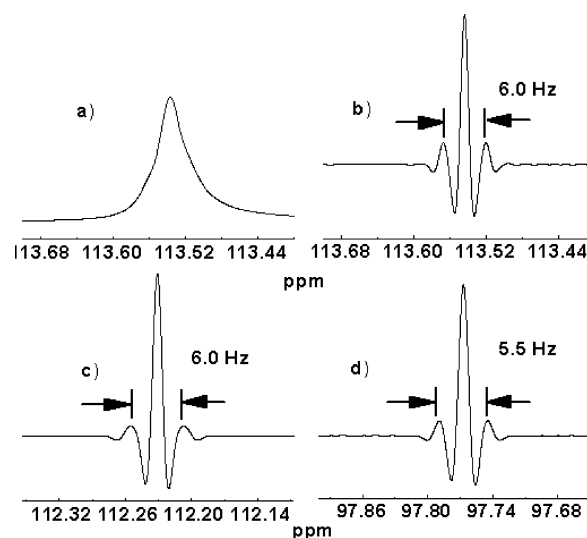


**Figure 10.** (a) Expanded  $^{13}\text{C}$  spectrum of resonance **x** shown in Figure 9 at  $113.5$  ppm with conventional line broadening,  $l = 1$  Hz. (b) Corresponding resonance **x** with negative line broadening applied ( $l = -5$ ,  $g = 0.25$ ). (c) Resonance **y** and (d) resonance **z** with negative line broadening applied ( $l = -5$ ,  $g = 0.25$ ).

The observed  $|J_{\text{SeSe}}|$  couplings are summarized in Table 1; the signs of these  $J$ -couplings are not known. In the  $^{77}\text{Se}$  spectrum, the satellites that are split by  $67\text{--}68$  Hz likely originate from  $^2J$  (Se–M–Se) coupling via one of the core metal atoms. The assignment as a homonuclear  $J$ -coupling is unambiguous in view of the results from the COSY experiment. Two-dimensional  $J$ -resolved spectroscopy revealed an additional pair of satellites (split by  $10\text{--}12$  Hz), but these were not completely resolved from the central singlet. Finally, the multiple-quantum (INADEQUATE) experiment validated this observation, resolving the  $J$ -coupled pair that had been occluded by the large singlet.

Other possible sources of  $J$ -coupling would arise from selenium coupling to rhenium ( $^{185}\text{Re}$ , 37% abundant, or  $^{187}\text{Re}$ , 62.9% abundant, both with  $I = 3/2$ ) or to osmium ( $^{187}\text{Os}$ ,  $I = 1/2$ , 1.6% abundant, or  $^{189}\text{Os}$ ,  $I = 3/2$ , 16.1%

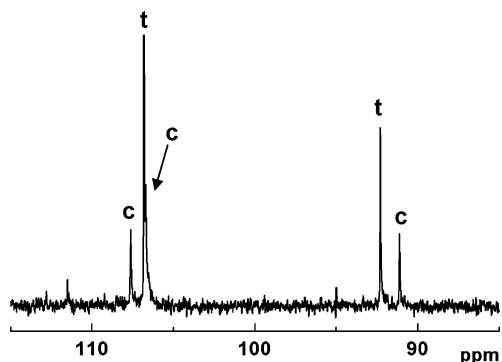


**Figure 11.**  $^{13}\text{C}$  spectrum of  $[\text{Re}_4\text{Os}_2\text{Se}_8(\text{CN})_6]^{2-}$  in DMF (without  $^1\text{H}$  decoupling). The resonances for the trans isomer are labeled with a “t” and those for the cis isomer with a “c.” Dominance of the trans isomer is evident in this spectrum. The most shielded resonances are those bound to osmium.

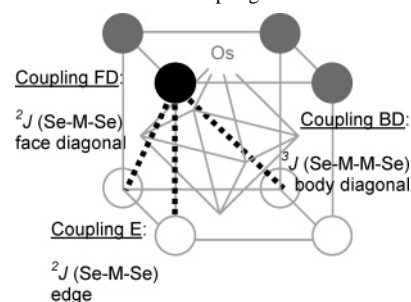
**Table 1.** *J*-Coupling Interactions Present in  $[\text{Re}_5\text{OsSe}_8(\text{CN})_6]^{3-}$

species	<i>J</i> -coupling	
$J_{\text{SeSe}}$	$ ^2J(\text{Se-M-Se}) $	66–68 Hz
	$ ^2J(\text{Se-M-Se}) $	10–11 Hz
$J_{\text{SeC}}$	$^{13}\text{C}$ bound to Re only, $^{77}\text{Se}$ on $\text{Re}_3$ faces	$ ^2J(\text{Se-Re-C}) $ ~6.0–6.7 Hz
	$^{13}\text{C}$ bound to Re, $^{77}\text{Se}$ on $\text{Re}_2\text{Os}$ faces	$ ^2J(\text{Se-Re-C}) $ ~5.4–5.6 Hz
$J_{\text{SeC}}$	$^{13}\text{C}$ bound to Os, $^{77}\text{Se}$ on $\text{Re}_2\text{Os}$ faces	$ ^2J(\text{Se-Os-C}) $ 4.8 Hz

abundant). However, these sources can all be ruled out on the basis of the splitting pattern and the intensities of the *J*-coupled peaks. The quadrupolar nuclei most likely relax too rapidly to allow for efficient spin–spin coupling to a neighboring selenium atom. The rapid spin–lattice relaxation of quadrupolar spins (which is generally true in liquids) averages out the *J*-coupling interactions to other spins in the same molecule. In general, the condition  $|2\pi J_{jk} T_1^k| \ll 1$  is satisfied for a quadrupolar nucleus in liquids.<sup>17</sup> Also possible is coupling of selenium to carbon ( $^{13}\text{C}$ ), but comparison of data from a  $^{13}\text{C}$ -labeled sample to one with natural abundance indicates that Se–C coupling, while present, is smaller than 10 Hz.

**Origin of the Observed *J*-Couplings (Calculation of Multiplet Intensities).** Examination of the structure of the  $[\text{Re}_5\text{OsSe}_8]^{3+}$  cluster core reveals that there are three different spin–spin interactions for the two-spin system (see Scheme 1; gray lines are provided as guides to the eye, not to imply associative interactions). Considering the black sphere to be one of the two NMR-active spins, there are three possible sites (shown in gray) for the second spin on the “top” of the cluster that would *not* result in *J*-coupling since they are chemically equivalent. There are four sites on the bottom half of the cluster that would, however, give rise to *J*-coupling interactions, shown as black dashed lines. One of these sites is directly beneath the black sphere along an edge of the  $\text{Se}_8$  cube, for which there is a  $^2J(\text{Se-M-Se})$  coupling, here referred to as an **E** (edge) interaction. Two sites are across a face diagonal from the black sphere (referred to as **FD**), also giving rise to a  $^2J(\text{Se-M-Se})$  coupling. Finally, the last site is across the body diagonal

**Scheme 1.** Possible Se–Se *J*-Coupling Interactions



from the black sphere, giving rise to a  $^3J(\text{Se-M-M-Se})$  interaction, referred to as **BD**.

Given our data, the weak satellites coupled by 10–11 Hz are assigned to coupling between spins along an edge (**E**) and the satellites coupled by 66–68 Hz are assigned to coupling along a face diagonal (**FD**). The resonances corresponding to body diagonal coupling (**BD**) are not observed.

We have assigned the observed *J*-coupled satellites through a simple statistical analysis of these sites and their relative populations in the  $\text{Re}_5\text{Os}$  cluster samples. As noted earlier, 34.9% of the synthesized clusters will have only one  $^{77}\text{Se}$  spin that is NMR-active, while 10.0% of the clusters will have two NMR-active spins. Only 1.64% of the clusters will have three NMR-active spins, and the remaining balance of the clusters (53.5%) will have no NMR-active selenium nuclei. (Cases of four or more spins are statistically insignificant.)

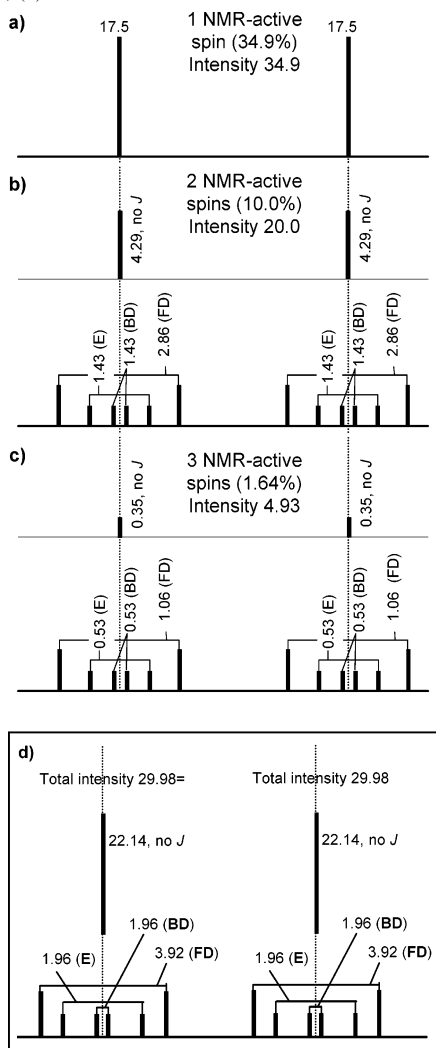
These percentages can be used as a measure of relative intensity as follows. Samples with one NMR-active  $^{77}\text{Se}$  nucleus will have an integrated intensity of 34.9 for the entire spectrum (i.e.,  $34.9\% \times 1$  spin), the two-spin samples will have a relative intensity of 20.0 (equivalent to  $10.0\% \times 2$  spins), and the three-spin samples will have a relative intensity of 4.92 (equivalent to  $1.64\% \times 3$  spins). The three-spin samples cannot be ignored because their intensity (4.92) is 8.22% of the total observed intensity.

First, we consider the case with just one NMR-active spin (integrated intensity of 34.9). Here, there will be no *J*-coupling, and the resulting spectrum should feature two singlets of equal intensity centered at the resonance for each type of selenium site, as shown in Scheme 2a. This one-spin case with a total integrated intensity of 34.9 will therefore have two resonances with intensities of  $\sim 17.45$  each.

Now consider a cluster with two NMR-active spins (integrated intensity of 20.0). From all possible combinations of two spins distributed among eight sites, a total of 12 out of 28 outcomes have two spins paired in chemically equivalent sites, in other words, without *J*-coupling: 6 of the 28 outcomes have the two  $^{77}\text{Se}$  nuclei associated only with the  $\text{Re}_2\text{Os}$  faces and another 6 have both NMR-active spins associated only with the  $\text{Re}_3$  faces. Each of these situations will produce singlets with intensities of 4.29 ( $=6/28 \times 20.0$ ) without *J*-coupling, centered at the isotropic chemical shifts,  $-188.6$  and  $-284.0$  ppm. The two resulting resonances are shown in Scheme 2b, labeled as “no *J*.” (See

(17) Levitt, M. H. *Spin Dynamics: Basics of Nuclear Magnetic Resonance*; John Wiley and Sons: West Sussex, 2001; p 225.

**Scheme 2.** Statistical Calculation of  $^{77}\text{Se}$  NMR Signal Intensities for (a) 1-Spin, (b) 2-Spin, and (c) 3-Spin Clusters, Including  $J$ -Coupling Interactions; (d) Is the Summation of All Three Cases



Supporting Information for details on how the different statistical outcomes were determined.)

A total of 8 out of 28 outcomes result in two spins associated by a **FD** interaction between chemically inequivalent sites. An **FD**-coupled pair of spins will result in two doublets, each centered about the isotropic resonance, and with each doublet having an integrated intensity of 2.86 ( $=4/28 \times 20.0$ ) (see Scheme 2b).

Coupling via the body diagonal (**BD**) is possible for only 4 out of the 28 outcomes; likewise, coupling via an edge (**E**) is possible for only the remaining 4 out of 28 outcomes. **BD**-coupling will result in two doublets, centered about the isotropic resonance with each doublet having an integrated intensity of 1.43 ( $=2/28 \times 20.0$ ), labeled as  $^3J$ . Similarly, **E**-coupling interactions will result in two doublets, centered about the isotropic resonance with each doublet having an integrated intensity of 1.43, labeled as  $^2J$ . These two interactions can be distinguished by their different coupling strengths (i.e., the magnitude of the satellite splittings, as shown schematically in Scheme 2b).

The three-spin cases are even more complex, with up to two coupling interactions (**E**, **BD**, **FD**) between each set of

three spins. There are 56 possible outcomes for distributing three spins among the eight selenium sites; the net result is shown in Scheme 2c.

To assign specific couplings, the 66–68 Hz coupled satellites in the Bloch decay spectra were fit using the Bayesian program and integrated, resulting in areas ranging from 11% to 12% of the total area of the entire resonance multiplet (i.e., central resonance plus satellites). Since only one set of satellites is clearly resolved in the Bloch decay spectra, their identity can be assigned on the basis of examination of their area with respect to the other features.

Assuming the 11 Hz-coupled satellites—evident in the 2D  $J$ -resolved and double quantum coherence experiments—are occluded by the large singlet resonance in the Bloch decay spectra, the central feature would then have a combined area of the non- $J$ -coupled features, as well as those satellites with  $J$ -couplings too small to resolve. As shown in Scheme 2d, the total intensity of each multiplet is 29.98; therefore, we are seeking any pair of  $J$ -coupled satellites whose area is  $\sim 11$ –12% of this total. Only the **FD**-coupled satellites come close to this integrated intensity, with  $(3.92/29.98) \times 100\% = 13.1\%$ . Either the **E**-coupled or **BD**-coupled pairs would yield an intensity of  $6.5\% = (1.96/29.98) \times 100\%$ . While the sum of **E**- and **BD**-coupled satellites would also yield 13.1%, there is no reason to believe that these two interactions (one is a  $^2J_{\text{Se-M-Se}}$  and the other a  $^3J_{\text{Se-M-M-Se}}$ ) should exhibit equal coupling strengths of 66–68 Hz.

Therefore, on the basis of the fitted data for the pair of outer satellites, the **FD**  $^2J$  interactions have a coupling strength of  $67 \pm 1$  Hz and produce the single pair of resolved satellites in the Bloch decay spectrum. The **BD** and **E**  $J$  interactions are occluded by the central feature in the Bloch decay spectra; however, at least one of these can be resolved through other methods. One can rationalize that the 11 Hz coupled pair of satellites observed is most likely an **E** interaction, as opposed to the **BD** interaction, since the **BD** coupling requires a long-range coupling via two different metals on the central  $\text{Re}_5\text{Os}$  core and would therefore most likely be the weaker of the two.

The different couplings, 67 and 11 Hz, are therefore both presumed to be  $^2J_{\text{Se-M-Se}}$  interactions, and it is interesting that the edge association results in a much smaller coupling strength than that of the face diagonal, where the  $J$ -coupled spins are obviously further away from each other. Clearly, these are both two-bond interactions (Se–M–Se) mediated by one of metal atoms at the center of the cluster; however, the geometric relationship between these two sites is not equivalent (the face diagonal being a factor of 1.414 longer than an edge).

Instances of Se–Se  $J$ -coupling interactions are somewhat rare. A study on  $\text{Se}_4\text{I}_4^{2+}$  and  $\text{Se}_6\text{I}_2^{2+}$  cations used similar types of  $^{77}\text{Se}$ – $^{77}\text{Se}$   $J$ -couplings to assist in discrimination between structures,<sup>18</sup> but in light of the results presented here, different assignments of the  $J$ -coupling interactions are possible. It is not intuitive that a more distant selenium species could yield

(18) Carnell, M. M.; Grein, F.; Murchie, M.; Passmore, J.; Wong, C.-M. *J. Chem. Soc. Chem. Commun.* **1986**, 225–227.



a stronger  $J$ -coupling, and the authors made their assignments conventionally, assigning the strongest coupling in the cubelike  $\text{Se}_6\text{I}_2^{2+}$  complex to the closest selenium atoms. Isotopic labeling of this material with  $^{77}\text{Se}$  could yield a definitive answer and would provide some insight as to whether these  $\mu_3$ -bonded selenium species we report here exhibit unique spin–spin coupling interactions or whether alternative assignments could be made in these earlier studies.

The  $^2J$  interactions reported here have analogues in the literature of organoselenides,<sup>2</sup> where it has been reported that Se–Se  $^2J$  and  $^3J$  couplings are sensitive to the overlap between lone pair orbitals. For example, these through-space interactions give a strong angular dependence to the coupling, and further investigations might demonstrate whether there is a similar driving force in these  $\mu_3$ -bonded systems.

The relative contributions of the orbital, spin-dipolar, and Fermi contact interactions are difficult to determine for heavy nuclei such as selenium, where relativistic effects must be taken into account, especially for direct Se–Se interactions.<sup>19</sup> However, for many systems (including those where relativistic effects can be ignored), the Fermi contact contribution to spin–spin coupling is considered to be the dominant factor in determining its magnitude, which is proportional to the  $s$ -electron density at the coupled nuclei. Generally, the magnitude of  $J$ -coupling interactions can be correlated in terms of the Pople–Santry expression:<sup>20</sup>

$$J_{AB} = \frac{h}{9\pi^2} (\gamma_A \gamma_X) \mu_0^2 \mu_X^2 \psi_A(0)^2 \psi_X(0)^2 \pi_{AX}$$

where  $\gamma$  is the gyromagnetic ratio for nuclei A and X,  $\mu_0$  is the permeability of free space,  $\mu_B$  is the Bohr magneton,  $\psi_A(0)^2$  and  $\psi_X(0)^2$  are the valence  $s$  electron densities at each nucleus, and  $\pi_{AX}$  is the mutual polarizability of the A and X  $s$  orbitals. Efforts are underway to calculate these three different  $J$ -coupling pathways to estimate their sign and magnitude.

**Assignment of Resonances via NMR of  $[\text{Re}_5\text{OsSe}_8(\text{CN})_6]^{3-}$  and  $J_{\text{C-Se}}$  Coupling.** The NMR resonances in the  $^{77}\text{Se}$  spectrum are unambiguously assigned through observation of  $J_{\text{C-Se}}$  couplings in the  $^{13}\text{C}$ -labeled sample. Recall that in the  $^{77}\text{Se}$  Bloch decay spectrum the deshielded multiplet centered at  $-188.6$  ppm is assigned to the  $\mu_3$ -Se atoms capping the  $\text{Re}_2\text{Os}$  triangular faces, while the shielded multiplet at  $-284.0$  ppm is assigned to those capping the  $\text{Re}_3$  faces.

These assignments are confirmed by the  $^{77}\text{Se}$  spectrum of  $[\text{Re}_5\text{OsSe}_8(\text{CN})_6]^{3-}$ . The Bloch decay spectra show slightly different  $J$ -coupled satellites arising from different  $^2J$  ( $^{77}\text{Se}$ –M– $^{13}\text{C}$ ) couplings for the two sites (see Figure 8). Selenium is coupling to three nearly equivalent neighbors, which in this case are the cyanide ligands bound to the three rhenium atoms of the triangular face it caps. These three neighboring carbon atoms cause the  $^{77}\text{Se}$  resonance to be

split approximately into a 1:3:3:1 quartet, with a  $^2J$  ( $^{77}\text{Se}$ –Re– $^{13}\text{C}$ ) coupling of 6.0–6.7 Hz.

In contrast, the deshielded resonance at  $-186.6$  ppm has a multiplet pattern that appears less symmetric. The large central resonance is still resolvable as being split into four features, but the splittings are less regular. Selenium is coupled here to two cyanide ligands bound to rhenium and one cyanide ligand bound to osmium; accordingly, what is observed is a less well-defined multiplet. The splitting of the inner two features is 4.8 Hz, but the two shoulder features are not easily resolved. The apparent pattern is consistent with a doublet of triplets, where the  $J$ -couplings are only slightly different from one another, and the outer peaks are split off from the central pair by 5.4–5.6 Hz. The  $^2J$  (Se–Os–C) coupling is assigned to the central 4.8 Hz coupled pair, and  $^2J$  (Se–Re–C) to the outer 5.5 Hz coupled set.

Observation of the  $^{13}\text{C}$  spectrum (Figure 10) provides confirmation of the  $J$ -couplings when negative line broadening has been applied. The spectrum displays three resonances, consistent with one cyanide ligand bound to the osmium site, four to the equatorial rhenium sites, and one to the axial rhenium atom located trans to osmium. When negative line broadening was applied to these spectra, satellites became evident for all three resonances. Notably, resonances **x** and **y** are close in chemical shift, and their  $^2J(\text{C–Re–Se})$  satellites are equivalent at  $\sim 6.0$  Hz. The third, shielded resonance is that of cyanide bound to osmium, and the concomitant  $^2J(\text{C–Re–Se})$  satellites are smaller at  $\sim 5.5$  Hz. It is worth noting that negative line broadening distorts the lines in such a way that these splittings cannot be evaluated with high precision. However, even though the magnitude of the coupling interactions is slightly different between the  $^{77}\text{Se}$  spectra and the  $^{13}\text{C}$  spectra, the general trend appears to be the same, with the osmium-mediated coupling being smaller than the rhenium-mediated coupling.

## Conclusions

In this study, it has been shown that octahedral metal clusters with multiple selenium sites exhibit both homonuclear and heteronuclear  $^{77}\text{Se}$   $J$ -couplings which can be utilized to assign resonances. A strategy of applying several well-known NMR techniques such as 1D double-quantum coherence (INADEQUATE) and 2D  $J$ -resolved spectroscopy has been set forth to characterize the homonuclear  $^{77}\text{Se}$ – $^{77}\text{Se}$  couplings. Knowledge of these  $J$ -couplings will be useful for interpreting  $^{77}\text{Se}$  data from different geometric isomers in systems with multiple selenium sites, and the NMR strategy that was set forth may assist other researchers studying polychalcogenides to seek out these couplings.

We have analyzed the clusters,  $[\text{Re}_5\text{OsSe}_8(\text{CN})_6]^{3-}$  and  $[\text{Re}_4\text{Os}_2\text{Se}_8(\text{CN})_6]^{2-}$ , via solution phase  $^{77}\text{Se}$  NMR. Statistical analyses of different spin–spin interactions allowed the two sets of  $J$ -coupled satellites to be assigned in the  $[\text{Re}_5\text{OsSe}_8(\text{CN})_6]^{3-}$  system. Two different  $^2J$  (Se–M–Se) couplings were measured on a single cluster, related to one another through interactions across a face diagonal or along an edge of the cube of inner selenium ligands. The edge association resulted in coupling of a smaller magnitude, even though

(19) Jameson, C. J. *Phosphorus-31 NMR Spectroscopy in Stereochemical Analysis*; VCH Publishers: New York, 1987; Chapter 6.

(20) Pople, J. A.; Santry, D. P. *Mol. Phys.* **1964**, *8*, 1–18.

the spins are further apart across the face diagonal. To the best of our knowledge, this is the first report of Se–Se spin–spin interactions for  $\mu_3$ -bonded selenium atoms in an octahedral metal cluster and is an example of rarely observed  ${}^2J({}^{77}\text{Se}–\text{M}–{}^{77}\text{Se})$  coupling through a transition metal, M.

**Acknowledgment.** We thank Dr. André d’Avignon, Mr. P. Curtis Carey, and Mr. Eric J. Welch for experimental assistance and Dr. G. Larry Bretthorst for his assistance with

Bayesian signal analysis. This material is based upon work supported by the National Science Foundation under Award No. CHE-0239560 and the Department of Energy under Award No. DE-FG03-01ER15257.

**Supporting Information Available:** Examples of two- and three-spin couplings. This material is available free of charge via the Internet at <http://pubs.acs.org>.

IC061571G